Performance-limiting factors for GaAs-based single nanowire photovoltaics

Xufeng Wang,[1,*] Mohammad Ryyan Khan,[1] Mark Lundstrom,[1] and Peter Bermel[1]

[1]*Birck Nanotechnology Center and School of Electrical and Computer Engineering, Purdue University, West Lafayette, IN 47907, USA*

[*]*wang159@purdue.edu*

Abstract: GaAs nanowires (NWs) offer the possibility of decoupling light absorption from charge transport for high-performance photovoltaic (PV) devices. However, it is still an open question as to whether these devices can exceed the Shockley-Queisser efficiency limit for single-junction PV. In this work, single standing GaAs-based nanowire solar cells in both radial and vertical junction configurations is analyzed and compared to a planar thin-film design. By using a self-consistent, electrical-optically coupled 3D simulator, we show the design principles for nanowire and planar solar cells are significantly different; nanowire solar cells are vulnerable to surface and contact recombination, while planar solar cells suffer significant losses due to imperfect backside mirror reflection. Overall, the ultimate efficiency of the GaAs nanowire solar cell with radial and vertical junction is not expected to exceed that of the thin-film design, with both staying below the Shockley-Queisser limit.

OCIS codes: (250.5590) Quantum-well, -wire and -dot devices; (350.6050) Solar energy; (040.5350) Photovoltaic.

References and links

1. M. A. Green, "Third generation photovoltaics: Ultra-high conversion efficiency at low cost," Prog. Photovolt. Res. Appl. **9**(2), 123–135 (2001).
2. J. Wallentin, N. Anttu, D. Asoli, M. Huffman, I. Aberg, M. H. Magnusson, G. Siefer, P. Fuss-Kailuweit, F. Dimroth, B. Witzigmann, H. Q. Xu, L. Samuelson, K. Deppert, and M. T. Borgström, "InP nanowire array solar cells achieving 13.8% efficiency by exceeding the ray optics limit," Science **339**(6123), 1057–1060 (2013).
3. W. Shockley and H. J. Queisser, "Detailed Balance Limit of Efficiency of p-n Junction Solar Cells," J. Appl. Phys. **32**(3), 510 (1961).
4. O. D. Miller, E. Yablonovitch, and S. R. Kurtz, "Strong Internal and External Luminescence as Solar Cells Approach the Shockley–Queisser Limit," IEEE J. Photovoltaics **2**(3), 303–311 (2012).
5. M. A. Green, K. Emery, Y. Hishikawa, W. Warta, and E. D. Dunlop, "Solar cell efficiency tables (version 42)," Prog. Photovolt. Res. Appl. **21**(1), 827–837 (2013).
6. B. M. Kayes, H. Nie, R. Twist, S. G. Spruytte, F. Reinhardt, I. C. Kizilyalli, and G. S. Higashi, "27.6% Conversion efficiency, a new record for single-junction solar cells under 1 sun illumination," in *IEEE Phovoltaic Specialist Conference*, (IEEE, 2011), 000004–000008.
7. P. Krogstrup, H. I. Jørgensen, M. Heiss, O. Demichel, J. V. Holm, M. Aagesen, J. Nygard, and A. Fontcuberta i Morral, "Single-nanowire solar cells beyond the Shockley–Queisser limit," Nat. Photonics **7**(4), 306–310 (2013).
8. T.-H. Her, R. J. Finlay, C. Wu, S. Deliwala, and E. Mazur, "Microstructuring of silicon with femtosecond laser pulses," Appl. Phys. Lett. **73**(12), 1673 (1998).
9. D. M. Callahan, J. N. Munday, and H. A. Atwater, "Solar Cell light trapping beyond the ray optic limit," Nano Lett. **12**(1), 214–218 (2012).
10. J. Zhu, Z. Yu, G. F. Burkhard, C.-M. Hsu, S. T. Connor, Y. Xu, Q. Wang, M. McGehee, S. Fan, and Y. Cui, "Optical AbsorptionEnhancement in Amorphous Silicon Nanowire and Nanocone Arrays," Nano Lett. **9**(1), 279–282 (2009).
11. L. Cao, P. Fan, A. P. Vasudev, J. S. White, Z. Yu, W. Cai, J. A. Schuller, S. Fan, and M. L. Brongersma, "Semiconductor nanowire optical antenna solar absorbers," Nano Lett. **10**(2), 439–445 (2010).
12. M. D. Kelzenberg, D. B. Turner-Evans, B. M. Kayes, M. A. Filler, M. C. Putnam, N. S. Lewis, and H. A. Atwater, "Single-nanowire Si solar cells," in *IEEE Photovoltaic Specialist Conference*, (IEEE, 2008), 1–6.
13. E. C. Garnett and P. Yang, "Silicon nanowire radial p-n junction solar cells," J. Am. Chem. Soc. **130**(29), 9224–9225 (2008).

#202402 - $15.00 USD Received 3 Dec 2013; revised 31 Jan 2014; accepted 3 Feb 2014; published 14 Feb 2014

14. E. C. Garnett, M. L. Brongersma, Y. Cui, and M. D. McGehee, "Nanowire Solar Cells," Annu. Rev. Mater. Res. **41**(1), 269–295 (2011).
15. B. M. Kayes, H. A. Atwater, and N. S. Lewis, "Comparison of the device physics principles of planar and radial p-n junction nanorod solar cells," J. Appl. Phys. **97**(11), 114302 (2005).
16. E. C. Garnett, C. Peters, M. Brongersma, Y. Cui, and M. McGehee, "Silicon nanowire hybrid photovoltaics," in *2010 35th IEEE Photovoltaic Specialists Conference*, (IEEE, 2010), 000934–000938.
17. M. M. Adachi, M. P. Anantram, and K. S. Karim, "Core-shell silicon nanowire solar cells," Sci. Rep. **3**, 1546 (2013).
18. J. Nelson, *The Physics of Solar Cells*, Series on Properties of Semiconductor Materials (Imperial College Press, 2003), Vol. 50, pp. 363–363.
19. F. Stern and J. M. Woodall, "Photon recycling in semiconductor lasers," J. Appl. Phys. **45**(9), 3904 (1974).
20. E. Yablonovitch, O. D. Miller, and S. R. Kurtz, "A great solar cell also needs to be a great LED: External fluorescence leads to new efficiency record," AIP Conference Proc. **9**, 9-11 (2013).
21. X. Wang, M. R. Khan, M. A. Alam, and M. Lundstrom, "Approaching the Shockley-Queisser limit in GaAs solar cells," in *IEEE Photovoltaic Specialists Conference*, (IEEE, 2012), 002117–002121.
22. U. Rau, "Superposition and Reciprocity in the Electroluminescence and Photoluminescence of Solar Cells," IEEE J. Photovoltaics **2**(2), 169–172 (2012).
23. X. Wang and M. S. Lundstrom, "On the Use of Rau's Reciprocity to Deduce External Radiative Efficiency in Solar Cells," IEEE J. Photovoltaics **3**, 1–6 (2013).
24. A. David, "High efficiency GaN-based LEDs: light extraction by photonic crystals," Ann. Phys. (Paris) **31**(6), 1–235 (2006).
25. E. Yablonovitch, "Inhibited Spontaneous Emission in Solid-State Physics and Electronics," Phys. Rev. Lett. **58**(20), 2059–2062 (1987).
26. S. C. H. Allen Taflove, *Computational Electrodynamics* (Artech House, 2005).
27. A. F. Oskooi, D. Roundy, M. Ibanescu, P. Bermel, J. D. D. Joannopoulos, and S. G. Johnson, "Meep: A flexible free-software package for electromagnetic simulations by the FDTD method," Comput. Phys. Commun. **181**(3), 687–702 (2010).
28. M. Bass, C. DeCusatis, J. Enoch, V. Lakshminarayanan, G. Li, C. MacDonald, V. Mahajan, and E. Van Stryland, *Handbook of Optics, Third Edition Volume IV: Optical Properties of Materials, Nonlinear Optics, Quantum Optics (set)*, Handbook of Optics (Mcgraw-hill, 2009).
29. Synopsys Sentaurus Semiconductor TCAD Software, East Middlefield Road, Mountain View, CA 94043 USA.
30. R. Pierret, *Semiconductor device fundamentals* (Addison-Wesley Publishing Company, 1996).
31. W. van Roosbroeck and W. Shockley, "Photon-Radiative Recombination of Electrons and Holes in Germanium," Phys. Rev. **94**(6), 1558–1560 (1954).
32. S. M. Durbin, J. L. Gray, R. K. Ahrenkiel, and D. H. Levi, "Numerical modeling of the influence of photon recycling on lifetime measurements," in *IEEE Phovoltaic Specialists Conference*, (IEEE, 1993), 628–632.
33. S. M. Durbin and J. L. Gray, "Numerical modeling of photon recycling in solar cells," IEEE Trans. Electron. Dev. **41**(2), 239–245 (1994).
34. J. Zhao and M. A. Green, "Optimized antireflection coatings for high-efficiency silicon solar cells," IEEE Trans. Electron. Dev. **38**(8), 1925–1934 (1991).
35. D. N. Wright, E. S. Marstein, and A. Holt, "Double layer anti-reflective coatings for silicon solar cells," in *IEEE Photovoltaic Specialists Conference*, (IEEE, 2005), 1237–1240.
36. X. Wang, M. R. Khan, J. L. Gray, M. A. Alam, and M. S. Lundstrom, "Design of GaAs Solar Cells Operating Close to the Shockley–Queisser Limit," IEEE J. Photovoltaics **3**(2), 737–744 (2013).
37. J. Moore, C. J. Hages, N. Carter, R. Agrawal, M. Lundstrom, and W. Lafayette, "The Physics of V bi -Related IV Crossover in Thin Film Solar Cells: Applications to Ink Deposited CZTSSe," in *IEEE Photovoltaic Specialists Conference*, 2013)
38. S. H. Demtsu and J. R. Sites, "Effect of back-contact barrier on thin-film CdTe solar cells," Thin Solid Films **510**(1-2), 320–324 (2006).
39. G. Lush and M. Lundstrom, "Thin film approaches for high-efficiency III-V cells," Solar Cells **30**(1-4), 337–344 (1991).

1. Introduction

It is commonly understood that with the advent of low-cost, moderate efficiency photovoltaics, the long-term future of photovoltaics, sometimes called the 'third generation,' would combine low costs with substantially higher efficiencies [1]. Nanowire solar cells can potentially satisfy both requirements and, as a result, are emerging as one of the most promising possibilities. To date, nanowire array solar cells have reached an efficiency of 13.8% [2]. The experimentally obtained efficiencies so far are still well below the Shockley-Queisser (SQ) limit—the ultimate theoretical efficiency limit for solar cells [3]. For GaAs-based single-junction photovoltaics, the SQ limit is at 33.5% [4], and the highest efficiency obtained today is at 28.8% under 1-Sun with a thin-film design [5, 6]. Thus, there is still a lot

#202402 - $15.00 USD Received 3 Dec 2013; revised 31 Jan 2014; accepted 3 Feb 2014; published 14 Feb 2014

of room for improvement, and nanowire array solar cells offer one possible approach. Since a single GaAs-based nanowire solar cell was recently reported to have an apparent solar conversion efficiency of 40% [7], there is an open question as to whether performance at this level could also extend to large-area arrays.

Nanowire-based solar cells certainly have some distinct advantages over the more traditional, planar solar cell designs. For example, nanowires display excellent light absorption with minimal reflection [8, 9]. In an array configuration, the wire diameter, spacing, and even shape can be optimized, and an effective broadband sunlight absorption as high as ~98% can be achieved [10]. In single standing nanowires with diameters comparable or less than the wavelength of incoming light, the effective light capture cross section can well exceed the wire's physical cross section. In other words, such nanowires can function as optical antennas and exhibit a "self-concentrating" effect [11]. This effect is primarily responsible for the high short-circuit current (J_{SC}) observed in [7]. One additional benefit is the amount of material saved. With 10 times self-concentration, nanowires ideally would require 10 times less material than thin film designs at the same absorption efficiency [12]. This potentially can drive down the material costs for manufacturing solar cells, while keeping the cell efficiency high. Another advantage is the added junction area in a radial-junction nanowire, where the p-n junction runs along the axis of the nanowire. Carriers generated inside the nanowire can be quickly collected by the junction without much diffusion [13–15], thereby improving the carrier collection efficiency.

On the other hand, nanowire solar cells also have some inherent disadvantages. One of the most obvious is their high surface-to-volume ratio. If left untreated, the nanowire surfaces can be defective with dangling bonds and as a result, induce large surface recombination. This is commonly cited as the leading cause for the low open-circuit voltages (V_{OC}) observed in fabricated nanowire solar cells [15–17]. However, this can be an advantage for certain applications such as electrochemical cells which require a high surface area-to-volume ratio. A second challenge associated with nanowires is building proper barriers for deflecting minority carriers away from contacts, such as the back-surface-field (BSF) used in silicon and GaAs thin-film solar cells [18]. Without proper minority carrier deflectors, the recombination loss at contacts can be significant. A third, lesser-known disadvantage is the decrease of reabsorption of radiated photons —a phenomenon known as photon recycling [19]. This has been shown to be a particularly important effect in high efficiency solar cells such as the GaAs double-heterostructure thin-film solar cells [6, 20, 21]. Near the SQ limit, radiative recombination becomes the dominant loss mechanism by emitting photons out of the device structure from recombined electron-hole pairs. If emitted photons can be trapped within the device and reabsorbed before escaping, they are not lost, so the radiative recombination is effectively decreased. Of course, one cannot completely eliminate the re-emission required by detailed balance. In planar solar cells, photon recycling benefits from having a backside mirror and total internal reflection, meaning only a small fraction of the isotropically emitted photons can escape the structure through the semiconductor (for GaAs, refractive index n=3.3 near the band edge)-air (n=1) interface. In comparison, nanowire solar cells are commonly designed to enhance in-coupling of light for maximum sunlight absorption, and as a result of reciprocity [22, 23], the radiatively emitted photons can also be extracted out of the device efficiently, thus decreasing the probability of reabsorption.

The design and operation of the nanowire solar cells are distinctly different, and arguably more complex than traditional solar cells. In traditional solar cells, the electrically active part of the cell, namely the p-n junction responsible for separating the carriers, is well separated from the optically active part, namely the anti-reflective coating for enhancing sunlight absorption. One can easily optimize one separately without too much concern for the other. In the nanowires however, the electrically and optically active regions are the same and one. Aspects such as photon recycling further complicate the design by linking the electrical transport with optical reabsorption. Thus, in order to properly predict the performance of

#202402 - $15.00 USD Received 3 Dec 2013; revised 31 Jan 2014; accepted 3 Feb 2014; published 14 Feb 2014

nanowire solar cells, one must consider the optical and electrical aspects in a self-consistent fashion. Moreover, photon recycling is an important aspect in devices other than nanowires also, for example, in optoelectronic devices such as LED [24]. We expect that, as the solar cell efficiency increases toward its ultimate limit, the complication of photon recycling linking electrical and optical components will become an important issue that is common to all the devices.

This paper explores practical issues of GaAs-based standing nanowire solar cell efficiency using detailed numerical simulations that include both electrical transport and optics. The first step, therefore, is to build a numerical device simulator including photon recycling in a way that is consistent with electrical transport. The details of our self-consistent electrical-optical model are discussed in Sec. 2. In Sec. 3, we first establish a baseline radial-junction nanowire structure as a starting point. We investigate both the radial and vertical junction designs in detail and compare their performance to a more traditional planar GaAs thin-film solar cell modeled after the current efficiency record at 28.8%. Our conclusions are summarized in Sec. 4.

2. Numerical methods

As discussed in Sec. 1, to properly model a nanowire solar cell, the electrical and optical aspects need to be considered in a self-consistent manner. The key physical phenomena included in our model are as follows:

- *Sunlight absorption (optics module)*: The absorption from sunlight must be properly modeled in 3D using wave optics solving Maxwell's equations.
- *Electrical transport (electrical module)*: The electron and hole transport equations coupled with Poisson's equation must be solved self-consistently in a 3D nanowire geometry. Due to the symmetry of the nanowire however, the equations can be solved in cylindrical coordinates.
- *Spontaneous emission (optics module)*: The spontaneous emission rate inside a nanowire can be very different from one under a homogenous environment [25]. Maxwell's equations need to be solved in 3D to resolve this spontaneous emission modification due to the nanowire geometry.
- *Photon recycling (optics module)*: The emission from the intrinsic radiative recombination has a finite probability to be reabsorbed, and this spatially-resolved absorption rate can be obtained, along with the spontaneous emission modification factor, by monitoring the divergence of the Poynting vector in the dispersive semiconductor material.

Below, we consider the implementation of both the optics and electrical modules, before moving on to our approach to integrating them together.

2.1 Optics module

For optical simulation in 3D nanowires, we employ a finite-difference time-domain (FDTD) simulation [26] implemented via a freely available software package developed at MIT, known as MEEP [27]. We have developed an optics module based on MEEP that delivers three quantities in matrix form: the sunlight absorption matrix, the spontaneous emission matrix, and the photon recycling matrix.

For the sunlight absorption matrix, the standard AM1.5G solar spectrum is used. The spectrum is first divided into 100 wavelength ranges, with each segment having 1/100 of the total sunlight flux. The average wavelength for each segment is used to characterize that particular segment. For each segment, one FDTD simulation is then done by injecting continuous-wave (CW), half TE and half TM, perpendicularly incident radiation onto the standing nanowire structure. To capture material dispersion, the GaAs is modeled with a

#202402 - $15.00 USD Received 3 Dec 2013; revised 31 Jan 2014; accepted 3 Feb 2014; published 14 Feb 2014

complex dielectric constant that depends on wavelength [28]. The absorption rate at each position can be obtained with the following formula [26]

$$P_{abs} = -0.5\omega|E|^2 \, imag(\epsilon), \tag{1}$$

where ω is the angular frequency, E is the complex electric field, and $imag(\epsilon)$ is the imaginary part of the dielectric constant associated with loss. The absorption rate is then weighted by the AM1.5G solar spectrum and summed over all the wavelengths.

For the spontaneous emission matrix and the photon recycling matrix, a dipole source is placed inside nanowire for the calculation. Virtual flux planes surrounding the nanowire, plus the integrated absorption within the nanowire, yield the total emission of the dipole. The same simulation is then done in a homogenous environment with the semiconductor material occupying the entire simulation space. The ratio between the amounts of the two emissions is the spontaneous emission modification factor inside a nanowire. The spatially resolved absorption inside the nanowire also gives us the photon recycling profile for radiative emission at that particular location. This photon-recycling rate is normalized to quantify, for one unit of emission at one position, what percentage (in units of /cm^{3}s) is reabsorbed at every other position. Of course, these simulations must be done at all the locations within the nanowire and for all dipole orientations (since no preferred direction is assumed). For each dipole orientation, the photon-recycling and emission enhancement profile throughout the nanowire does not have continuous rotational symmetry. For this reason, the optical module, unlike the electrical module to be discussed next, must be done in 3D instead of in cylindrical coordinate.

2.2 Electrical module

For electrical simulations of nanowires, we use Sentaurus from Synopsys [29] which solves the semiconductor transport equations coupled with Poisson's equation self-consistently in 1D, 2D, and 3D [30]. For this study, we exploit the fact that electrical transport in nanowires has continuous rotational symmetry about the wire center, and use cylindrical coordinates to reduce computational time. Various recombination mechanisms are considered in this study, including the bulk SRH, surface, Auger, and radiative recombinations. Important material parameters are listed below in Sec. 3.1, where a baseline nanowire structure is established.

Radiative recombination is an intrinsic property of any piece of material at a finite temperature, and in a homogeneous environment, it is related to the absorption coefficient by the Roosbroeck-Shockley equation [31],

$$R_{emit}(V=0) = \int R_{emit}(v)dv = \int \frac{8\pi v^2 n^2}{c^2} \frac{\alpha(v)}{e^{(hv/kT)}-1} dv, \tag{2}$$

where $\alpha(v)$ is the optical absorption coefficient at wavelength v, n is the index of refraction, T is the material temperature, and h, c, and k are standard physical constants. The condition where the applied voltage $V = 0$ indicates this equation applies at equilibrium. Away from equilibrium, the quasi-Fermi levels for electrons and holes split, so that:

$$R_{emit}(V) = R_{emit}(V=0)e^{qV/kT}. \tag{3}$$

The spatially resolved spontaneous emission modification factor, calculated from the optics module, is then used to scale this intrinsic radiative recombination rate. Subsequently, the photon recycling matrix is used to calculate the reabsorption, and this introduces a new generation term into the continuity equation for electrical transport calculations in Sentaurus.

#202402 - $15.00 USD Received 3 Dec 2013; revised 31 Jan 2014; accepted 3 Feb 2014; published 14 Feb 2014

2.3 Electro-optically coupled simulator

The overall flow of the electro-optically coupled simulator is shown in Fig. 1. Sentaurus conveniently offers Physical Model Interfaces (PMI) to allow seamlessly integration with the optical module. The optical module is parallelized. An entire simulation for one standing nanowire with ~400 nm in diameter and ~2 μm in length takes approximately 5 hours with 100 cores (64-bit, dual 12-core AMD Opteron 6172). A similar electro-optically coupled approach based on ray-tracing optics and 1D transport has been successfully used in the past to investigate GaAs solar cells approaching the SQ limit [32, 33].

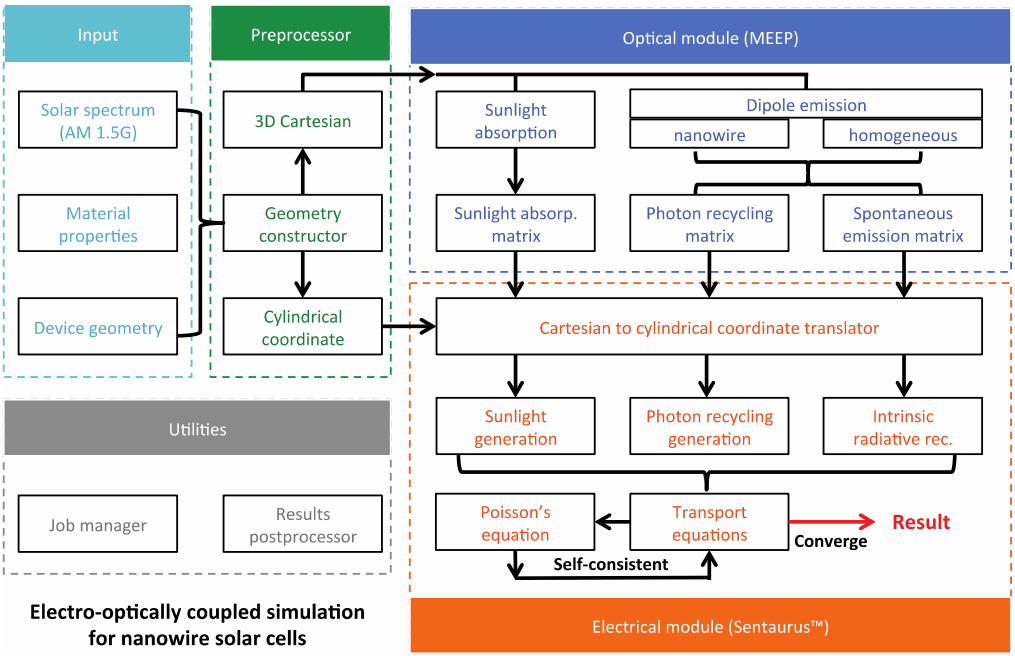

Fig. 1. Electro-optically coupled simulation framework flowchart, suitable for incorporating photon recycling effects into a PV device simulation in a self-consistent fashion.

3. Results and discussion

3.1 Baseline parameters and performance

To compare various designs and parameters, a baseline nanowire solar cell is modeled after [7]. The device structure is shown in Fig. 2(a). The single standing nanowire is GaAs-based with a radial junction. It is 212.5 nm in radius and 2.5 μm in height. It stands on a p-type doped silicon substrate. At its center is a $7x10^{18}$ /cm^3 p-type doped GaAs core with 147.5 nm radius. An intrinsic GaAs layer of 15 nm radial thickness is sandwiched between the p-type core and a $7x10^{18}$ /cm^3 n-type doped GaAs shell. The heavily doped p-type substrate is assumed to make an ideal Ohmic contact with the p-type GaAs core, and the n-type contact is only in contact with the top of the nanowire and is transparent. These are of course very ideal assumptions, but doing so allows us to independently control the surface recombination velocities on the side. We concern only the intrinsic losses of the solar cell design (surface and bulk SRH, Auger, radiative recombinations, etc.). We do not take extrinsic factors into account (shadowing, series resistance, front reflection, reliability, grid design, etc.). The temperature is set to 300 K. In this work, we focus on this specific nanowire geometry and compare its radial and vertical junction configurations with thin-film design. The optimization of such solar cells and the performance in array settings will be investigated in a later study. In addition, although, as pointed out in [7], the structure is not optimized for maximum

#202402 - $15.00 USD Received 3 Dec 2013; revised 31 Jan 2014; accepted 3 Feb 2014; published 14 Feb 2014

efficiency, it provides us a realistic platform to start our numerical study. Although the performance may differ with different device dimension or material parameters, the detailed physics of the device operation and observations made thereof remain the same.

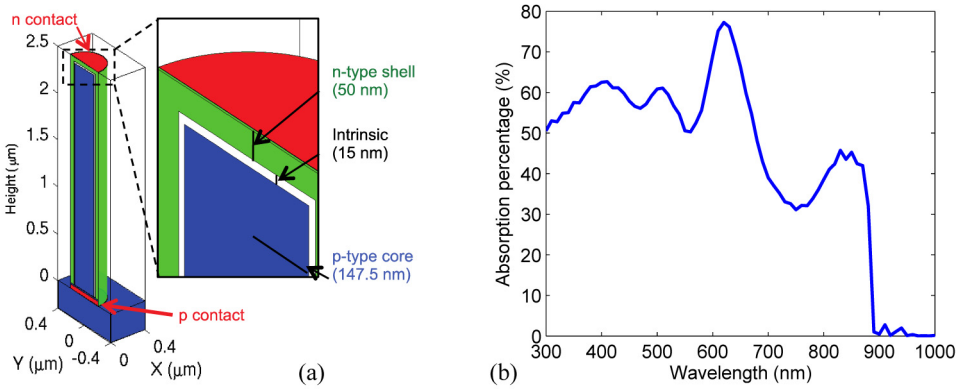

Fig. 2. (a) Baseline single nanowire solar cell geometry with a radial junction; (b) Absorptivity vs. incident wavelength for the baseline single nanowire solar cell.

Table 1. Key baseline material parameters[a]

	Electron	**Hole**
Mobility	2500 $cm^2/V{\cdot}s$	60 $cm^2/V{\cdot}s$
SRH lifetime	1 μs	1 μs
Auger coefficient	$7x10^{-30}$ cm^6/s	$7x10^{-30}$ cm^6/s
Effective density of states	$4.7x10^{17}$ $/cm^3$	$9x10^{18}$ $/cm^3$
Recombination velocity at contacts	10^7 cm/s	10^7 cm/s
Surface recombination velocity	10^7 cm/s	10^7 cm/s

[a] unless mentioned specifically, all simulations in this study use the parameters in this table by default.

The absorption percentage of perpendicularly incident CW light is plotted in Fig. 2(b). The absorptivity exhibits several peaks as the incident wavelength becomes comparable or exceeds the nanowire's physical diameter. The complete result for different diameters can be found in [7]. Overall, the broadband absorptivity for a single standing nanowire is much less than what one can achieve in an array of nanowires and in thin-films with multiple layers of anti-reflection coatings [34, 35].

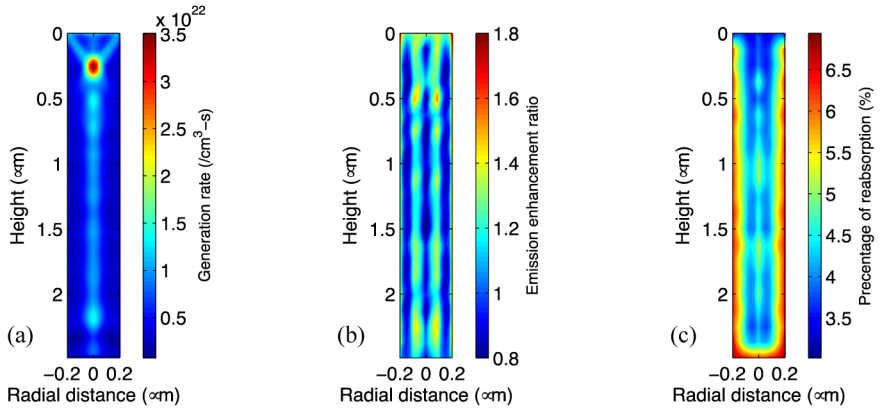

Fig. 3. Three important quantities are spatially resolved with wave optics simulation: (a) Carrier generation rate under AM1.5G. (b) Spontaneous emission enhancement with respect to a homogeneous environment. (c) Spatially resolved photon recycling probability.

#202402 - $15.00 USD Received 3 Dec 2013; revised 31 Jan 2014; accepted 3 Feb 2014; published 14 Feb 2014

Figure 3 shows the three important optical matrices generated by the wave optics module. Figure 3(a) shows the spatially resolved generation rate from AM1.5G sunlight spectrum. The generation focuses strongly at the center of the nanowire and away from the surfaces. This is beneficial, since a defective surface may rapidly recombine electron-hole pairs generated near its vicinity. Figure 3(b) shows the spatially resolved spontaneous emission modification factor. The overall modification to the spontaneous emission is not very significant for this particular nanowire. The result also shows invariance along the nanowire length. This is due to the fact that the aspect ratio of the wire is large, so it can be approximated as a wire with infinite length. The solution is not expected to vary along the length in an infinite wire. Figure 3(c) shows the spatially resolved percentage of reabsorption. It is interpreted as the percentage of photon emission reabsorbed by the nanowire, after averaging over x, y, and z dipole orientations. The average photon recycling probability is only around ~5% for this particular nanowire structure. This is in stark contrast with a well-designed thin-film solar cell, where more than 80% of the emission can be recycled [5, 6, 36] – more than an order of magnitude higher. This small photon recycling in nanowires is the consequence of having improved light coupling, which enhances the emission by reciprocity. For this reason, photon recycling in single GaAs nanowire photovoltaic is low and may even be disregarded without introducing much error. On the other hand, photo recycling in planar GaAs solar cells can be significant and shall not be disregarded. In general, to know the significance of photon recycling and emission enhancement for a novel nanostructure, it is important to conduct a full electro-optically coupled simulation as we have demonstrated in this work.

This suppression of photon recycling due to enhanced out-coupling is an inherent disadvantage for nanowire solar cells. As suggested in [20], at open-circuit, the external luminescence efficiency should be as close to 100% as possible. For every photon absorbed from the incident spectrum, one should be "extracted" from the device. But to maximize open-circuit voltage, the quasi-Fermi level spitting must be maximized. This means that Δn should be as large as possible. The internal recombination rate, $\Delta n/\tau$, must equal the rate at which photons are absorbed from the incident illumination, G_{OP}. To maximize Δn, the carrier lifetime should be as long as possible. Non-radiative processes must be minimized so that the lifetime is dictated by photons emitted by radiative recombination that leave the cell. To make the lifetime as long as possible, we should make it **difficult** to extract the emitted photons using, for example, a planar thin-film solar cell with good backside mirror as illustrated in Fig. 3(b) of [4]. So there are two ways to achieve 100% luminescence efficiency: 1) extract the emitted photons quickly, but this results in low lifetime, low Δn, and low open-circuit voltage, or 2) make it hard for emitted photons to escape, which results in high lifetime, high Δn, and higher open-circuit voltage. Both approaches give 100% external luminescence efficiency, but the second is preferable for solar cells. To make the lifetime as long as possible, one should trap the photons emitted by radiative recombination inside the cell for as long as possible.

#202402 - $15.00 USD Received 3 Dec 2013; revised 31 Jan 2014; accepted 3 Feb 2014; published 14 Feb 2014

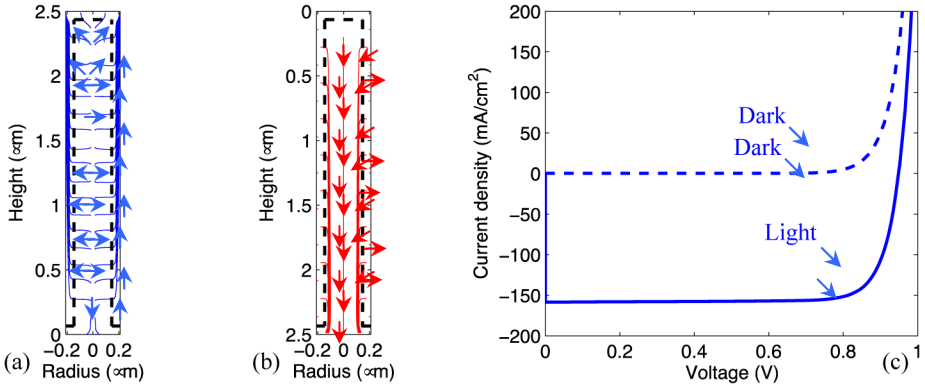

Fig. 4. With radial junction, (a) Electron current flow streamline at J_{SC}. (b) Hole current flow streamline at J_{SC}. (c) Benchmark single nanowire solar cell light and dark IV.

Once the electron-hole pairs are generated, each carrier will be set to motion in accordance with the transport equations and Poisson's equation. Figure 4(a) shows the flow of electrons inside the nanowire at J_{SC}. The core region is p-type, so the electrons generated in the core need to travel to the n contact at the top of the nanowire to be collected. As seen in Fig. 4(a), the radial junction is very effective in collecting the electrons. Electrons quickly travel radially to the nearest p-n junction and flows along the n-type shell toward the n contact at the top. Some of the electrons generated at the bottom of the nanowire recombined at the p contact. Figure 4(b) shows the flow of holes inside the nanowire at J_{SC}. Some of the holes generated inside the n-type shell are collected by the p-n junction, but the rest recombine at the surface (arrows pointing outward). However, since the generation of the carriers focuses away from the surface (Fig. 3(a)), the loss due to surface recombination is significantly reduced.

The light and dark IVs are shown in Fig. 4(c). The IVs shows typical solar cell behavior obeying the superposition principle [37]. Despite the poor absorptivity shown in Fig. 2(b), the optical antenna effect concentrates the light outside the physical cross-section of the nanowire and boosts its overall absorption. The total generation within the nanowire divided by its physical area is at 260 mA/cm^2. Due to recombination losses, primarily surface recombination and emission, the J_{SC} is reduced to 160 mA/cm^2. This J_{SC} is comparable to the experimentally reported value at 180 mA/cm^2 in [7]. On the other hand, the predicted V_{OC} is at 0.94 V, comparing to the experimentally reported value at 0.43 V. This large discrepancy is possibly due to defects such as shunts or series resistance. The simulation thus suggests the low V_{OC} observed is not fundamental to nanowire solar cells, and there is a lot of room for improvement through material and design optimization.

3.2 Nanowire solar cell with radial junction

We take a closer look at the role of surface recombination and electrical contacts in the nanowire solar cell with radial junction. Figure 5(a) shows the J_{SC} and V_{OC} under various surface recombination velocities. Any surface recombination velocity lower than 10^4 cm/s has minimal effect on the cell performance, while anything higher will lower both the J_{SC} and V_{OC}. The result suggests that, by treating the surfaces and removing dangling bonds, the single nanowire reported in [7] may obtain an extra J_{SC} of ~25 mA/cm^2. The major loss mechanisms at V_{OC} are shown in Fig. 5(b). Surprisingly, recombination at contacts can be significant when the surface recombination is not dominating. The contact recombination primarily comes from the diffusion of electrons generated inside the p-type core toward the back p-type contact. Such contact recombination can significantly degrade the performance of solar cells. A heavily doped back-surface-field (BSF) in silicon or a heterojunction in GaAs

#202402 - $15.00 USD Received 3 Dec 2013; revised 31 Jan 2014; accepted 3 Feb 2014; published 14 Feb 2014

thin-film solar cells is commonly used to deflect minority carriers away in order to minimize the contact recombination loss [38]. These types of structures however could be a significant challenge to implement experimentally in nanowire solar cells.

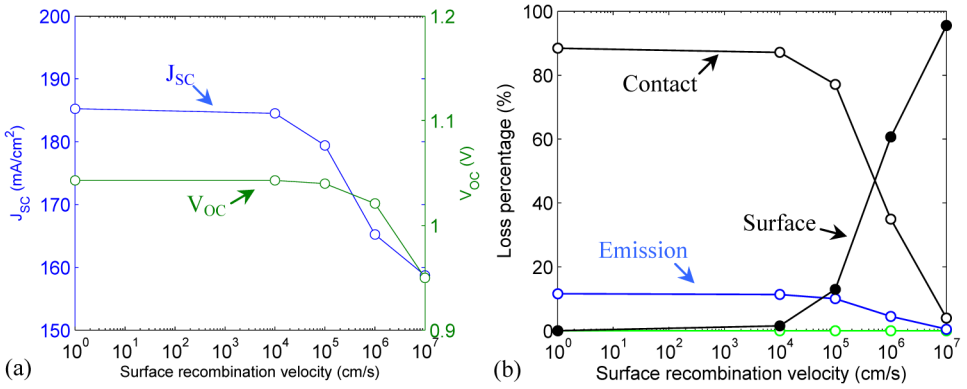

Fig. 5. With no minority carrier deflections at both contacts, performances for various surface recombination velocities are displayed. (a) J_{SC} and V_{OC}. (b) Percentage of each major loss mechanism at V_{OC}.

Figure 6(a) shows the solar cell performance under various surface recombination velocities assuming no contact recombination. An extra ~5 mA/cm^2 in J_{SC} and ~100 mV in V_{OC} could be obtained through improved minority carrier deflection at both contacts. When both the surface and contact recombination are low, the radiative recombination, labeled as "emission" in Fig. 6(b), becomes the dominant loss mechanism. The radiative recombination thus caps J_{SC} and V_{OC} at approximately 190 mA/cm^2 and 1.1 V respectively.

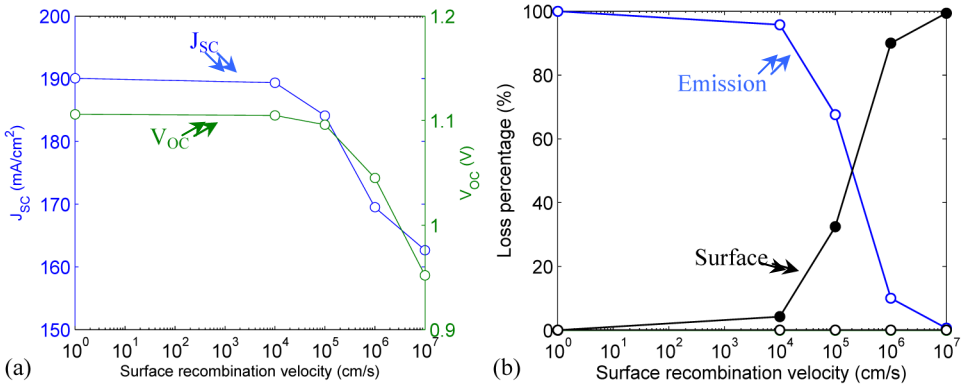

Fig. 6. With complete minority carrier deflection at both contacts, performances for various surface recombination velocities are displayed. (a) J_{SC} and V_{OC}. (b) Percentage of each major loss mechanism at V_{OC}.

3.2 Nanowire solar cell with vertical junction

In this section, we investigate an alternative design for the nanowire solar cell. In the vertical junction configuration, the p-i-n regions are stacked vertically along the nanowire height. The resulting geometry, as shown in Fig. 7(a), is effectively the radial junction structure with the side junction removed and everything else kept the same. The top vertical junction in fact exists in the radial junction structure, but it is not primarily responsible for the separation of charges—the side junction does this job and collects majority of the current. Now in the vertical junction configuration, with the side junction removed, the only place carriers can be separated is at the very top of the wire.

#202402 - $15.00 USD Received 3 Dec 2013; revised 31 Jan 2014; accepted 3 Feb 2014; published 14 Feb 2014

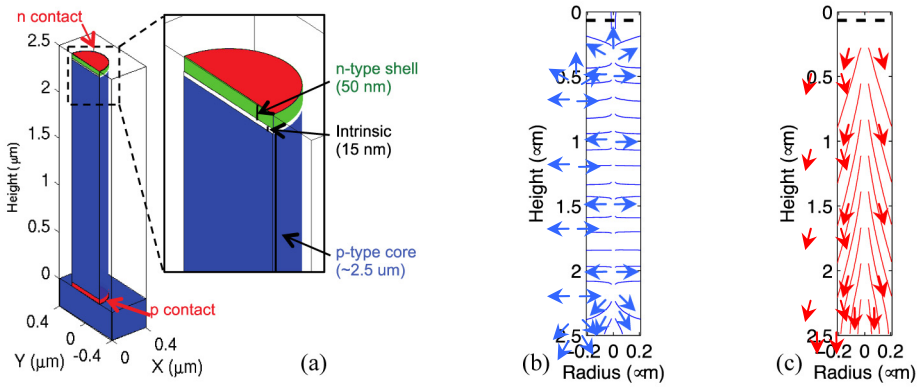

Fig. 7. With vertical junction, (a) Device geometry. (b) Electron current flow streamline at J_{SC}. (c) Hole current flow streamline at J_{SC}.

Figure 7(b) shows the electron current flow within the nanowire. Without the radial junction isolating the surfaces, the electrons generated in the p-type region quickly flow to the surface and recombine. Only a small fraction of the electrons that are generated near the vicinity of the depletion region at the top of the nanowire are collected. The surface recombination is so high that, as seen in Fig. 7(c), the hole current is significantly distorted as a result. Therefore, intuitively, one would expect the vertical junction is much more vulnerable to defective surfaces and, therefore, performs worse than the radial junction.

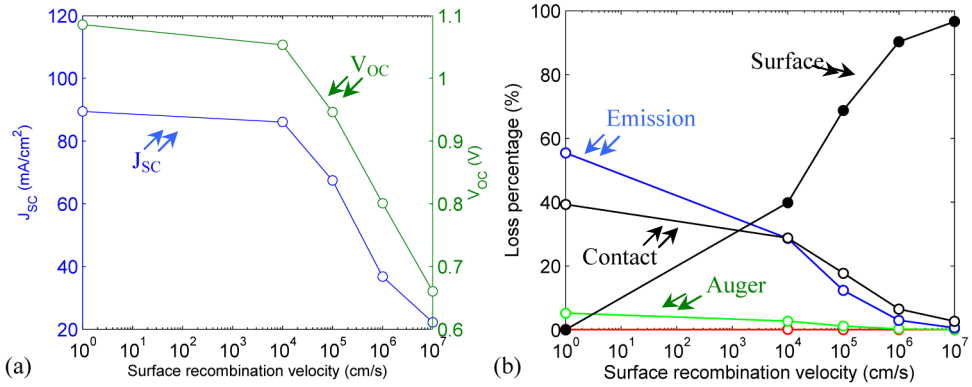

Fig. 8. With no minority carrier deflections at both contacts, performances for various surface recombination velocities are displayed. (a) J_{SC} and V_{OC}. (b) Percentage of each major loss mechanism at V_{OC}.

Figure 8(a) confirms the vertical junction's vulnerability to surface recombination. Overall, the J_{SC} and V_{OC} values are significantly lower than those for radial junctions. If the surfaces are left untreated, the J_{SC} can plummet to as low as 20 mA/cm^2, which is 1/13 of the total absorption. The V_{OC} can be significantly reduced as well. In this situation, materials having low surface recombination when left untreated, such as InP, become preferable to GaAs.

#202402 - $15.00 USD Received 3 Dec 2013; revised 31 Jan 2014; accepted 3 Feb 2014; published 14 Feb 2014

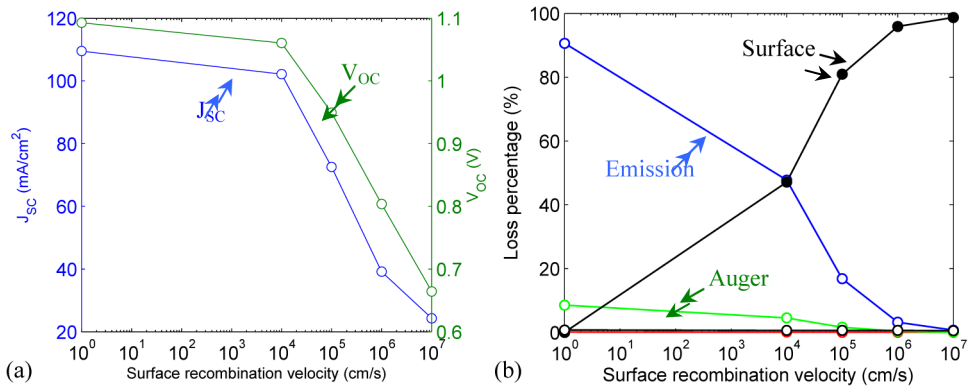

Fig. 9. With complete minority carrier deflections at both contacts, performances for various surface recombination velocities are displayed. (a) J_{SC} and V_{OC}. (b) Percentage of each major loss mechanism at V_{OC}.

Since contact recombination in the vertical junction is not the most dominant recombination at V_{OC}, one expects little effect on V_{OC} when the contacts are improved to deflect minority carriers, as shown in Fig. 9(a) and 9(b). On the other hand, the J_{SC} can be improved to gain ~20 mA/cm^2, suggesting significant electron diffusion toward the back contact. The J_{SC} in the best case is significantly lower than the one in the radial junction, due to the inefficient collection of carriers causing carriers to be lost through radiative emission. Over all, the vertical junction displays an inferior performance compared with the radial junction due to its vulnerability to surface defects and inefficient carrier collection.

3.4 Planar thin-film solar cell

High efficiency single-junction solar cells using GaAs have been created using a thin-film approach, with efficiencies as high as 28.8% under the standard solar spectrum being reported [36]. This efficiency is fairly close to the theoretically predicted SQ efficiency limit at 33%. The planar thin-film solar cell is less complex than a nanowire cell, and many theoretical studies have been done to investigate its physics. A more detailed design study of GaAs thin-film solar cells toward the SQ limit can be found in [36]. In this work, we only briefly look at the role of the backside mirror reflectivity to illustrate the major differences between nanowire and thin-film solar cells.

Figure 10(a) shows the thin-film solar cell geometry. It is equivalent to the vertical junction nanowire extended to have an infinite radius. The structure has two distinct features that nanowire cells do not have. One is the front and back AlGaAs/GaAs heterojunction interface blocking the minority carriers away from the contacts. This is a commonly deployed feature in thin-film cells, and therefore, we assume there is no minority carrier loss at the contacts. The other distinct feature is the backside mirror, which reflects the radiatively emitted photons back to the thin-film and enhances photon recycling. This effect has been known and proposed as a means to increase GaAs solar cell efficiency, going back to early work from over two decades ago [39].

In order to make a fair comparison with the nanowire geometry, the total generation rate in the planar cell is kept the same as that in nanowires. This translates to a 7.7-Sun concentration that produces a generation current of 260 mA/cm^2.

#202402 - $15.00 USD Received 3 Dec 2013; revised 31 Jan 2014; accepted 3 Feb 2014; published 14 Feb 2014

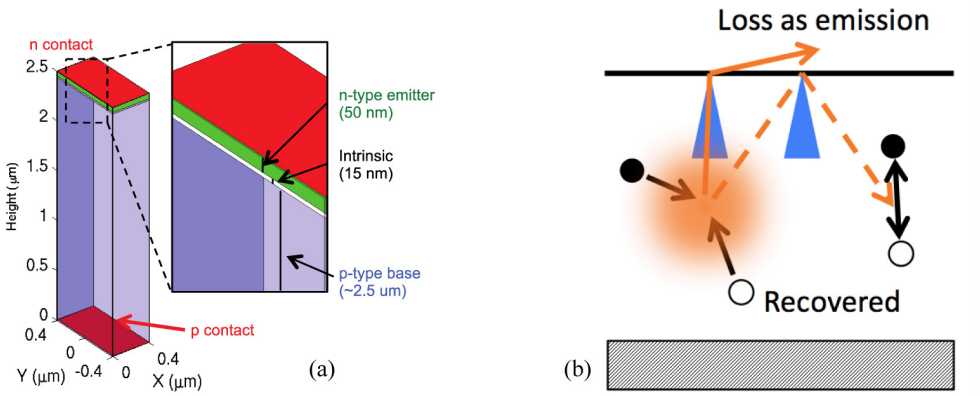

Fig. 10. (a) Thin-film solar cell geometry. (b) Illustration of photon recycling and emission inside a thin-film solar cell.

With the absence of surface and contact recombination, which are the two major sources of non-radiative recombinations in nanowires, the radiative recombination loss dominates in thin-film GaAs solar cells. This is an expected signature of any solar cell approaching its SQ limit, as non-radiative recombination losses are being minimized. The radiatively emitted photons, if not recycled, may be emitted out of the structure or be parasitically absorbed by the backside mirror. This is illustrated in Fig. 10(b). The planar semiconductor/air interface creates a small escape cone, allowing only ~2% of the emission escapes the structure. The rest of the emitted photons are trapped within the thin-film through total internal reflection, until they are reabsorbed by the semiconductor or parasitically absorbed by the mirror and turned into waste heat. The emitted photons concentrate closely to the bandgap energy, where the absorption probability is low for such photons. The photons thus need to bounce around the thin-film and travel an extended distance for recycling. A fraction of the photons striking the backside mirror are lost due to the imperfect reflectivity. Thus, as shown in Fig. 11, the mirror reflectivity noticeably influences both the J_{SC} and V_{OC}. Unless it is designed to have a high reflectivity (> 90%), the mirror is responsible for majority of the radiative recombination loss and thus is the bottleneck toward higher efficiency.

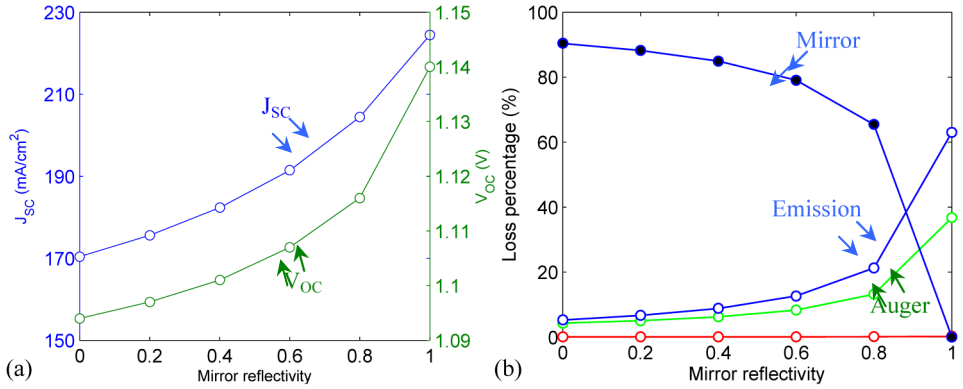

Fig. 11. With bulk SRH lifetime at 1 us, performances for various backside mirror reflectivities are displayed. (a) J_{SC} and V_{OC}. (b) Percentage of each major loss mechanism at V_{OC}.

3.4 Summary

Table 2 summarizes the best performing radial and vertical junction nanowire solar cells and planar solar cell seen in this study. Also listed are experimentally reported record efficiency

#202402 - $15.00 USD Received 3 Dec 2013; revised 31 Jan 2014; accepted 3 Feb 2014; published 14 Feb 2014

III-V solar cells. Due to the self-concentration effect, nanowires display an abnormally high apparent (uncorrected) efficiency exceeding 100%. We term this efficiency the "apparent efficiency" (Apparent η). Since this measure does not account for a mismatch between the optical collection area and geometric cross-sectional area, the simulated J_{SC} should be divided the self-concentration factor in order to calculate the effective efficiency (η). This effective efficiency is what would be observed after masking the optical input cross-sectional area to equal the geometric cross-sectional area; it is most suitable for comparison with other photovoltaic technologies. Note that the V_{OC} and Fill Factor (FF) are both assumed to stay invariant with concentration, since the concentration affects them only logarithmically, much less than J_{SC}.

Table 2. Performance comparison for various III-V single-junction solar cell types under 1-Sun, where shaded rows are numerical predictions in this study.

	Source	J_{SC} (mA/cm^2)	V_{OC} (V)	FF	Apparent η*	**η**
Radial junction single nanowire	[7]	180	0.43	0.52	40%	**5.2%**
	This work	190	1.1	0.84	175.6%	**25.1%**
Vertical junction single nanowire	This work	110	1.08	0.85	101%	**14.4%**
Nanowire array - vertical junction	[2]	24.6	0.779	0.724	-	**13.8%**
Planar bulk	[5]	29.8	1.030	0.86	-	**26.4%**
Planar thin-film	[5]	29.68	1.122	0.865	-	**28.8%**
	This work (7.7-Sun)	225	1.14	0.87	223.2%	**31.9%**
SQ limit	[3]	33.5	1.12	0.89	-	**33.5%**

* Apparent efficiency does not account for a mismatch in the collection area and geometric cross-sectional for nanowires exhibiting self-focusing effects, and thus is not a 'true' efficiency measure.

The reported single, radial junction, nanowire solar cell in [7] shows an efficiency at 5.2%, while the theoretically predicted performance may reach as high as 25.1%. This suggests that there is still a lot of room for improvement. In comparison, the vertical junction performs much worse with a theoretically predicted best efficiency at 14.4%. Interestingly, one of the highest efficiency nanowire array solar cells is made from vertical junction with InP at 13.8% efficiency [2]. As discussed in Sec. 3.3, one of the key disadvantages of vertical junctions is the lack of depletion region area to efficiently collect the carriers. Compared to the vertical junction structure we used in this study, the InP nanowire array has a much more optimal design. The intrinsic region extends throughout the majority of the wire length, creating a built-in electric field that separates the charges efficiently.

The fabricated planar bulk and thin-film solar cells, at 26.4% and 28.8% respectively, significantly outperforms the nanowire solar cells. As discussed in Sec. 3.4, having no side surfaces and using double-heterojunction structures are two of the key advantages that planar cells have over nanowire solar cells. The thin-film solar cell has an additional advantage in having a backside mirror to enhance photon recycling. The predicted best thin-film solar cell efficiency is at 31.9%. In comparison, the SQ limit is at 33.5%. The intriguing fact that the planar solar cell can exceed the V_{OC} of the SQ limit has been explained in detail in [4] and [36].

4. Conclusion

In this study, we used an electro-optically coupled simulator to investigate the performance of GaAs-based single NW solar cell with radial and vertical junctions, based on the experimental structure explored in [7]. The thin-film GaAs solar cell is used as a comparison to illustrate some of the important differences between NW and thin-film designs. Through an extensive set of numerical simulations, we showed that the low V_{OC} observed experimentally for the

#202402 - $15.00 USD Received 3 Dec 2013; revised 31 Jan 2014; accepted 3 Feb 2014; published 14 Feb 2014

NW cell at 0.43 V is not a fundamental limit; there is a lot of room for improvement to obtain higher efficiency in such cells. At V_{OC}, contact recombination becomes a major loss factor in radial junction design, while the vertical junction is much more vulnerable to surface defects. If both engineering challenges are addressed, NW solar cells can obtain high efficiencies comparable, but still lower, to that of thin-film solar cells. The distinct advantage of total internal reflection and backside mirror allows thin-films to exhibit better photon recycling. Single nanowires, on the other hand, have strong in-coupling and out-coupling of light, which creates the possibility of optical self-focusing, but also decreases photon recycling. Although the apparent efficiency can exceed 33%, this effect is caused by optical self-focusing. Thus, we found it is necessary to correct raw short-circuit currents observed by effectively masking the light entering to match the geometric cross-section of the nanowire. With this correction, near the SQ limit where radiative recombination dominates, nanowires demonstrate lower V_{OC} and J_{SC} values and efficiencies than a thin-film solar cell. Although the design principles differ, both the nanowire and thin-film solar cells are constrained by the same physical principles and neither should be expected to exceed the SQ limit.

Acknowledgments

The authors thank Professors Muhammad Ashraful Alam and Jeff Gray at Purdue University for helpful discussions, and Dr. Yeqing Lu at Synopsys for his patience and help in integrating PMI modules into Sentaurus. Support was provided by the Department of Energy, under DOE Cooperative Agreement No. DE-EE0004946 ("PVMI Bay Area PV Consortium"), as well as the Semiconductor Research Corporation, under Research Task No. 2110.003 ("Network for Photovoltaic Technologies").